

Development of a gas chromatography-based method to derive halogen bonding energy of At compounds

Katsuyuki Tokoi^a, Atsushi Toyoshima^{b,*}, Masashi Kaneko^a, Atsushi Shinohara^{b,c}, Yoshitaka Kasamatsu^a

^aGraduate School of Science, Osaka University, Toyonaka, Osaka 560-0043, Japan

^bInstitute for Radiation Sciences, Osaka University, Toyonaka, Osaka 560-0043, Japan

^cOsaka Aoyama University, Minoh, Osaka 562-8580, Japan

Received October 19, 2023; Accepted December 4, 2023; Published online January 10, 2024

Halogen bonding has attracted a great deal of attention in recent years due to its applications across various scientific fields. Halogen bonding of astatine (At) is theoretically predicted to be similar to that of iodine by taking into account relativistic effects. In this study, we developed a new method based on gas chromatography and aided by quantum calculations to derive halogen bonding energy (HBE) of At compounds. A different methodology was necessary because the usual spectroscopic methods for HBE determination are not suitable for limited trace quantities of At compounds. We determined the adsorption enthalpies (ΔH s) of aromatic halogen compounds on thiourea by the developed gas chromatography-based method. The relationship between ΔH and calculated HBEs was successfully obtained for halopentafluorobenzene and thiourea. We expect this relationship can be used to evaluate the HBE of astatopentafluorobenzene.

Keywords: halogen bonding, gas chromatography, quantum chemical calculation, Lewis base resin

1. Introduction

Halogen bonding has been widely utilized in molecular syntheses in various research endeavors including crystal engineering¹, organic chemical reactions², removal of halogenated compounds³, and design of pharmaceuticals⁴. This peculiar bonding of halogens is an intermolecular interaction between a positively polarized region on a halogen atom, which usually appears on the opposite side of its σ bond to such atoms as carbon, and a lone pair of a Lewis base (LB)⁵. The capability of fluorine (F), chlorine (Cl), bromine (Br), and iodine (I) for halogen bonding increases with increasing atomic polarization and decreasing atomic electronegativity⁶; the order is F < Cl < Br < I. However, there are few experimental reports that systematically investigate the halogen bonding properties. In particular, data on heavier halogens such as astatine (At) and tennessine (Ts) are very scarce. It is, therefore, very important to study these heavier halogens for deeper understanding of the halogen bonding.

In the periodic table of elements, At is placed under I. Based on trends in homologous elements, At is expected to have stronger halogen bonding than lighter halogens have. On the other hand, At is expected to be strongly influenced by relativistic effects. Galland *et al.*⁷ theoretically investigated the interaction energy of the halogen bonding between At₂ and ammonia and showed that the halogen bonding of At₂ is as strong as that of I₂ due to the spin-orbit interaction. Galland *et al.* reported the scalar relativity halogen bonding energy (HBE) of At₂ and ammonia to be -41 kJ/mol, whereas the HBE value considering the spin-orbit interactions was -32 kJ/mol. Thus, it is necessary to examine the influence of the spin-orbit interaction in the halogen bonding of At.

Spectroscopic methods are often used to determine the HBE which represents the strength of halogen bonding⁸. Because At

has only short-lived radioisotopes with the longest being ²¹⁰At (half-life of 8.1 h) and ²¹¹At (7.2 h), the available amount of At for research studies is typically limited to less than 10^{-12} mol. This restriction prevents the use of any spectroscopic techniques to study the HBEs of At compounds. Guo *et al.*⁹ and Liu *et al.*¹⁰ employed a solvent extraction method to determine the formation constants of complexes forming the halogen bonding between AtI and various LBs. From the comparison of their obtained constants ($\log K_{\text{BAtI}}$) with literature values for the corresponding formation constants of I₂ ($\log K_{\text{BI}_2}$), Guo *et al.*⁹ found the relationship between the two constants. They concluded that AtI has stronger halogen bonding than I₂. However, we consider it to remain uncertain whether the formation constants have a simple relationship with the HBE because the influence of solvation has not been taken into account.

In this paper, we developed a new derivation method of HBEs of At compounds in trace quantities that is based on the relationship between calculated HBE values and adsorption enthalpies (ΔH s) of lighter halogens which are experimentally obtained by gas chromatography. The ΔH is a measure of adsorption strength of compounds of interest onto a column surface in a gas phase and can be applied to small quantities of compounds¹¹. The ΔH involves van der Waals forces, dipoles, and hydrogen bonding¹². Lee *et al.*¹³ have explored the relation between the ΔH s of alkylamines (LB) on an acidic zeolite surface in which hydrogen bonding is involved and the proton affinities of the alkylamines that are an indicator of the ability of an LB to accept protons. They found a linear relationship between the ΔH s and the proton affinities. An analogous relationship can readily be thought to exist between halogen bonding and hydrogen bonding. Both interactions are based on an electron donor/electron acceptor relationship involving a halogen-like atom and an electron-dense counterpart⁵. Therefore, because proton affinity is similar to HBE, ΔH is expected to

*Corresponding author. E-mail: toyo@irs.osaka-u.ac.jp

have a linear relationship with HBE.

We describe our investigation of the relationship between calculated HBE and ΔH of lighter halogens for the purpose of developing a derivation method for HBE of At compounds by extrapolation. First, gas chromatography experiments using halogen compounds on a thiourea resin were carried out to determine their ΔH s. Thiourea was selected because it is expected to have strong halogen bonding¹⁰. HBEs of the corresponding complexes were then obtained using quantum calculations. To ensure the calculation accuracy, we compared the redshift of the C-X stretching vibration measured by Raman spectroscopy¹⁴ with the calculated results of the C-X stretching vibration. Finally, the relationship between the measured ΔH s and calculated HBEs was evaluated.

2. Experimental

2.1 Materials. Halopentafluorobenzene (C_6F_5X , X = Cl, Br, and I) and halobenzene (C_6H_5X) were purchased from Tokyo Chemical Industry Co. Hexane was purchased from Fujifilm Wako Pure Chemicals Co. All reagents are commercially available and they were used without additional purification. Thiourea supported on silica gel (Si-Thiourea resin, R69530B) was purchased from SiliCycle Inc. The Si-thiourea resin has a loading amount of 1.20 mmol/g and can be used at temperatures to 150°C.

2.2 Gas chromatography using LB resin. As studied samples, C_6F_5X and C_6H_5X were used because they are expected to exhibit strong and weak retentions on the LB Si-thiourea resin, respectively, according to their halogen bonding. A gas chromatograph (Shimadzu GC-2014) equipped with a thermal conductivity detector was used for the experiments. Teflon tubing (800 mm long, 3 mm inner diameter, and 5 mm outer diameter) was utilized as a column which was filled with the LB Si-Thiourea resin to a packed length of 500 mm. The sample inlet temperature was set to 160°C. The column temperature was kept at 140, 145, and 150°C during the experiments. Helium was chosen as a carrier gas with a flow rate of 10 mL/min. A syringe was employed to inject 4 – 12 μ L of a sample. The acquired chromatograms were fitted with the GaussMod function to determine the retention time¹⁵. The retention times here were expressed as follows

$$t'_r = t_r - t_m, \quad (1)$$

where t'_r is the adjusted retention time, t_r is the observed retention time, and t_m is the time through the empty column.

2.3 Raman spectroscopy. For the Raman spectroscopy measurements, a mixed sample of C_6F_5I and Si-Thiourea resin and a C_6F_5I sample were prepared. In a 1.5-mL polypropylene tube, 0.23 mmol of C_6F_5I and 98 mg of the Si-thiourea resin were mixed and kept at room temperature for 11 h. For the C_6F_5I sample, 200 μ L of C_6F_5I and 1600 μ L of hexane were mixed in a quartz measurement vial; the concentration of C_6F_5I was 0.84 M. Hexane was used as a solvent because it can dissolve C_6F_5I and has no peak in the energy range of interest in a Raman spectrum. Raman spectra were measured using a micro-Raman spectrometer (Jasco Co. NRS3100) with laser wavelength of 750 nm at room temperature. Each spectral point was measured 5 times with an exposure time of 60 s each.

2.4 Quantum chemical calculation. All quantum calculations were carried out using Gaussian 16 software¹⁶. Initial geometries of the molecules (C_6H_5X , C_6F_5X , and thiourea) and the donor-acceptor complexes with a ratio of 1:1 (C_6H_5X -thiourea and C_6F_5X -thiourea complexes) were constructed

using Gaussview 6.1¹⁷. Structures of all the compounds were optimized using the density functional theory calculation with the ω B97XD functional¹⁸, followed by single-point energy calculations using second-order Møller-Plesset perturbation theory (MP2). Aug-cc-pVDZ basis sets^{19,20,21} were employed for all atoms except iodine, and the DGDZVP basis set^{22,23} was assigned to iodine. The basis sets were employed for both the geometry optimization and single-point energy calculations. All the self-consistent field calculations were performed under tight convergence criteria, in which the tolerance of energy was set to 10^{-6} Hartree during the iterations. The HBE for each complex was calculated by using the total energies obtained in the single-point calculations, as shown in equation (2)

$$\text{HBE} = \{E^{\text{tot}}(\text{complex}) + E^{\text{tot}}_{\text{BSSE}}(\text{complex})\} - \{E^{\text{tot}}(\text{donor}) + E^{\text{tot}}(\text{acceptor})\} \quad (2)$$

Here E^{tot} denotes the total energy and $E^{\text{tot}}_{\text{BSSE}}$ is the correction term for the basis set superposition error based on the counterpoise method²⁴.

In the benchmark calculation, the computational conditions (e.g., basis set, calculation method) were optimized based on experimental HBE values for the CF_3Cl-NH_3 system⁸. Next, to evaluate the validity of the calculation conditions in the studied complex of C_6F_5I -thiourea, the peak positions of the Raman shift of the C-I bonding were calculated under the determined conditions and compared with experimental values. In the vibrational frequency calculation to obtain the Raman spectra, the solvent effect was taken into consideration using the polarizable continuum model (PCM) with the dielectric constant of the solvent²⁵.

3. Results and Discussion

3.1 Gas chromatography using the LB Si-thiourea resin.

Figure 1 shows a chromatogram of each compound obtained with a column temperature of 145°C. The obtained chromatograms were fitted as the red curves in Figure 1. Retention time was evaluated from the fitted peak. Figures 2 and 3 show the retention times of C_6F_5X and C_6H_5X , respectively, at various column temperatures. The decrease of retention time as a function of column temperature was fitted with equation (3)²⁶,

$$t'_r = \frac{A \times B \times L}{F} \exp\left(\frac{-\Delta H}{RT}\right), \quad (3)$$

where A is the interstitial area of the column (m^2), B is a constant (showing entropy change in adsorption), L is the length of the packing material (m), F is the flow rate (mL/min), ΔH is the adsorption enthalpy (kJ/mol), T is the column temperature (K), and R is the gas constant (J/mol K). Table 1 summarizes the calculated ΔH values of halogen compounds obtained using equation (3).

We observed an increasing variation of ΔH s for heavier halogens for C_6F_5X , which is consistent with the general trend of HBEs. On the other hand, C_6H_5X exhibited nearly identical ΔH values. Hogan *et al.*²⁷ calculated energies of hydrogen and halogen bonding between water and C_6H_5X and showed that hydrogen bonding is dominant over halogen bonding. This suggests a significant contribution of hydrogen bonding to adsorption behavior of C_6H_5X in the present study. Thus, we considered the observed nearly identical ΔH s of C_6H_5X originate from hydrogen bonding between C_6H_5X and silica gel. Since the C-F---H-O hydrogen bonding is weak, the involvement of hydrogen bonding in the ΔH of C_6F_5X is expected to be small²⁸.

3.2 Raman spectroscopy. Table 2 lists the Raman spectra peaks of C_6F_5I and of C_6F_5I adsorbed on Si-thiourea resin. A distinct peak at 207 cm^{-1} attributed to the C-I bond was

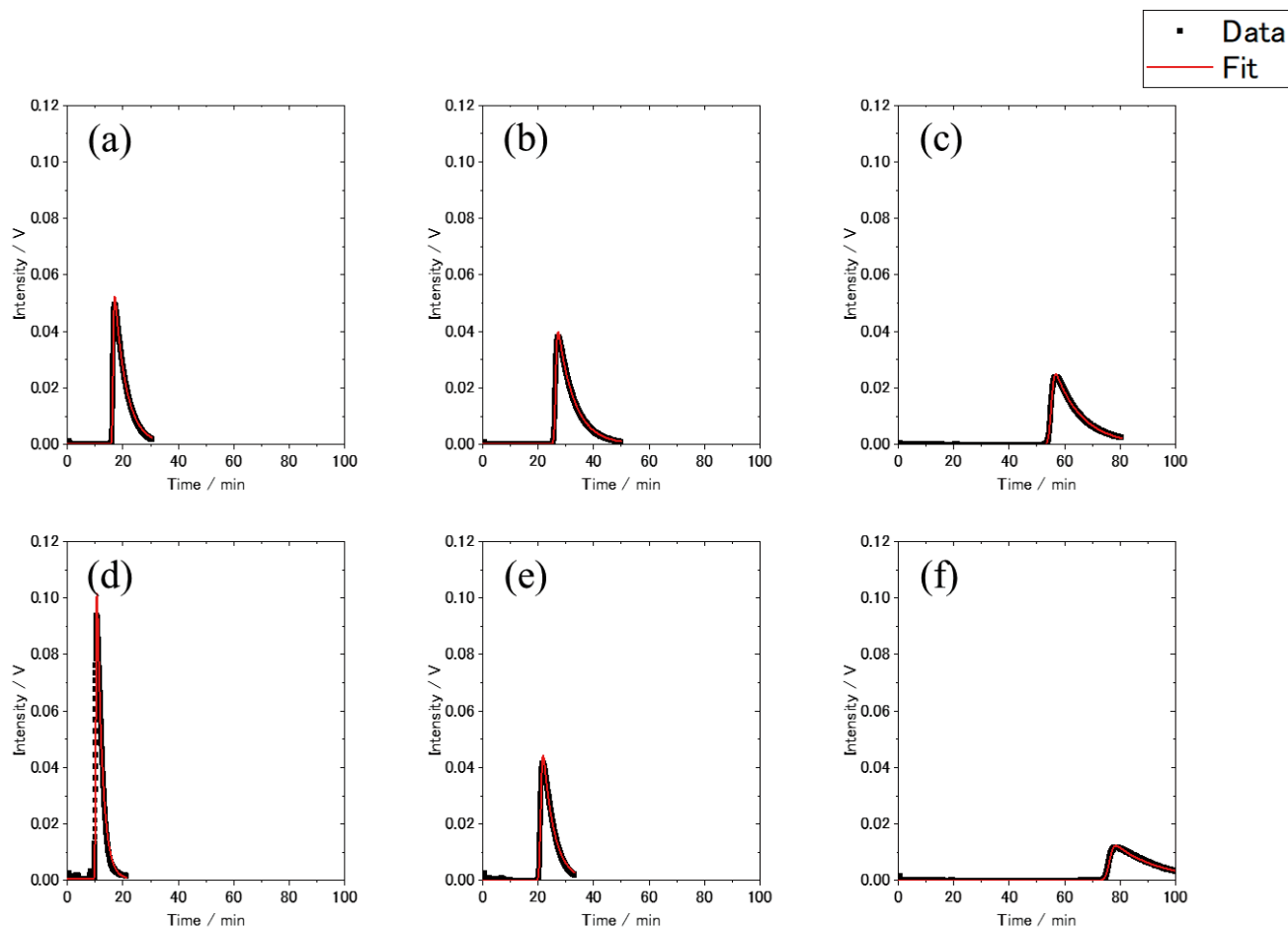


Figure 1. Chromatograms of each sample obtained at a column temperature of 145°C. (a) C_6H_5Cl , (b) C_6H_5Br , (c) C_6H_5I , (d) C_6F_5Cl , (e) C_6F_5Br , and (f) C_6F_5I . Red lines are fitted curves.

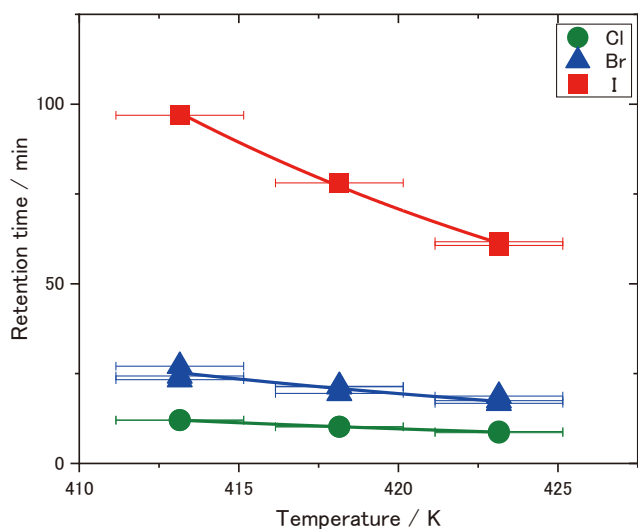


Figure 2. Variations of retention times of C_6F_5X ($X = Cl, Br, \text{ and } I$) as a function of column temperature. Each solid line represents the fitted curve.

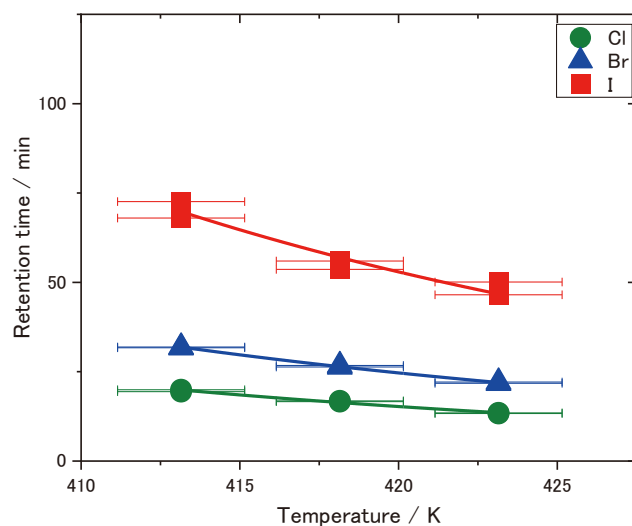


Figure 3. Variations of retention times of C_6H_5X ($X = Cl, Br, \text{ and } I$) as a function of column temperature. Each solid line represents the fitted curve.

TABLE 1: Calculated ΔH values for halogen compounds C_6F_5X and C_6H_5X .

Element	$\Delta H, \text{ kJ mol}^{-1}$	
	C_6F_5X	C_6H_5X
Cl	-47.0 ± 1.7	-56.0 ± 3.2
Br	-55.0 ± 7.5	-54.1 ± 1.4
I	-67.5 ± 2.3	-58.3 ± 7.9

TABLE 2: Experiment and quantum chemical calculation values of Raman peaks.

Samples	C-I Raman shift, cm^{-1}	
	Experiment	Calculation
C_6F_5I	207	208
C_6F_5I + thiourea resin	197	198 ^a

^a Calculations were performed on C_6F_5I -thiourea complex.

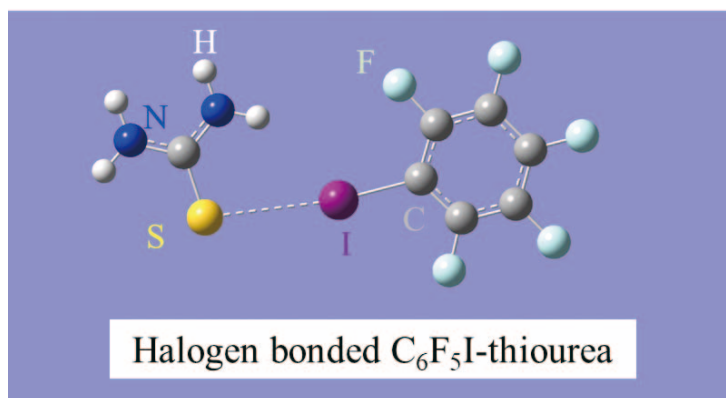


Figure 4. Structures of the halogen bonded C_6F_5I -thiourea complex obtained in the quantum chemical calculation.

TABLE 3: Optimized structures of C_6F_5X -thiourea and C_6H_5X -thiourea complexes.

Element	X-S distance, Å		C-X-S angle, °	
	C_6F_5X -thiourea	C_6H_5X -thiourea	C_6F_5X -thiourea	C_6H_5X -thiourea
Cl	3.538	— ^a	159.712	— ^a
Br	3.346	3.623	168.099	167.121
I	3.346	3.616	172.778	171.062

^aThe geometry optimization of C_6H_5Cl -thiourea failed to converge.

observed for the C_6F_5I sample. For the C_6F_5I sample adsorbed on the resin, the C-I peak was found at 197 cm^{-1} , indicating the redshift by the halogen bonding. Bramlett *et al.*²⁹ reported the C-I peak of C_6F_5I in dichloromethane was at 204 cm^{-1} . The slight discrepancy between the present value and the literature value²⁹ would be due to the different solvents of the measured samples³⁰.

3.3 Quantum chemical calculations. In determining the basis set conditions, benchmark calculations were performed using the HBE of $CF_3Cl \cdots NH_3$ measured in reference 8 which is -11.0 kJ/mol . Using aug-cc-pVDZ as the basis set at the MP2 level yielded HBE of -10.0 kJ/mol that well reproduced the reported experimental value⁸. We further verified that a close value was obtained with a structure optimized using $\omega B97XD$.

For the structure optimization and vibrational analysis with the $\omega B97XD$, aug-cc-pVDZ was used for non-iodine atoms, and DGDZVP was used for iodine atoms. The results are listed in Table 2. Under these calculation conditions, the peak positions of C-I, with and without thiourea, were 208 and 198 cm^{-1} , respectively. The experimental and calculated Raman spectra for this system were in a good agreement with each other, indicating that the present calculation conditions were reliably applied to the HBE calculations.

Figure 4 and Tables 3 and 4 give the results of structural optimization and HBE calculations conducted with the optimized conditions of the calculation method and basis sets. For C_6H_5Cl , HBE values were unavailable since the structural optimization did not converge, possibly due to the weaker nature of the halogen bonding ability of Cl compared to that of the other halogens.

Similar to previous findings³¹, the increase in HBE was observed as the atomic number of the halogen increased. C_6F_5X had a larger HBE due to the electron-withdrawing effect of the aromatic ring fluorine³¹.

TABLE 4: Results of HBE calculations based on quantum chemical calculations.

Element	HBE, kJ mol^{-1}	
	C_6F_5X -thiourea	C_6H_5X -thiourea
Cl	-15.9	—
Br	-20.1	-14.3
I	-24.8	-17.0

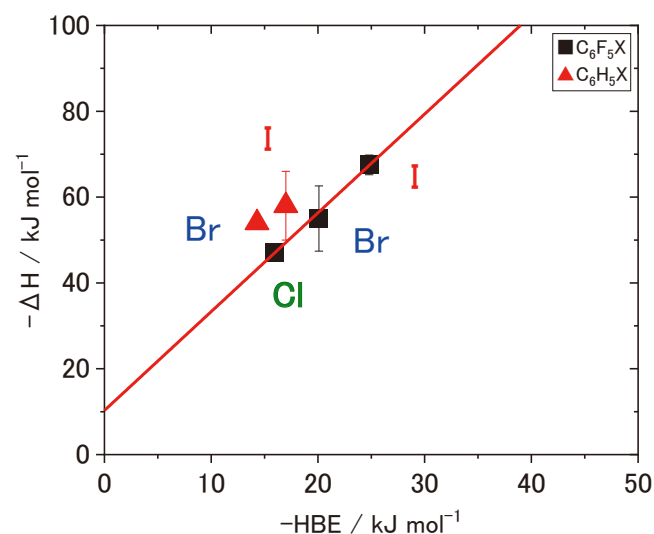


Figure 5. Relationship between ΔH s and HBEs of C_6F_5X and C_6H_5X ($X = Cl, Br,$ and I). The red line is the fitted straight line for the C_6F_5X data.

3.4 Relationship between ΔH and calculated HBE.

Figure 5 shows the relationship between ΔH s and calculated HBEs of our studied compounds. For C_6F_5X , ΔH s and calculated HBEs demonstrated a good linear relationship with the Pearson correlation coefficient of 0.9995. The fitted line is expressed as

$$\Delta H = (2.3 \pm 0.1) \times \text{HBE} + (10.4 \pm 1.4) \text{ kJ/mol.} \quad (4)$$

As observed in the earlier study¹³, a linear relationship was observed in the calculated HBE vs. ΔH in the present reaction system. The observed HBE dependence of ΔH suggests that halogen bonding contributes to the adsorption on the Si-thiourea resin. There are halogen bonding modes involving multiple LBs, which are known to increase calculated HBE compared to single halogen bonding³². Thus, the slope of equation (4) is considered to be greater than 1 because of the involvement of multiple halogen bonding interactions. In the next step, the investigation of multiple halogen bonding models with quantum chemical calculations should be involved. The value of the intercept is expected to represent the strength of interactions such as van der Waals forces without halogen bonding in ΔH . We, therefore, concluded that the HBE of C_6F_5X can be inferred from the ΔH value determined by gas chromatography, i.e., the equation of the relationship between ΔH and the calculated HBE in homologous elements may be used to evaluate the HBE of $C_6F_5\text{At}$.

4. Conclusion

The ΔH of C_6F_5X was determined through gas chromatography experiments utilizing a Si-thiourea resin as a Lewis base. The relationship between ΔH and HBE was successfully obtained. We expect the HBE value of astatopentafluorobenzene can be derived from its ΔH determined with gas chromatography using the developed methodology. By comparing the HBE value with that from relativistic quantum calculations, it may become possible to explore the influence of relativistic effects on the halogen bonding of At compounds.

Acknowledgements

This work was the result of using research equipment shared in the MEXT Project for promoting public utilization of advanced research infrastructure (Program for supporting construction of core facilities) Grant Number JPMXS0441200023. One author (KT) acknowledges financial support from the Multidisciplinary Ph.D. Program for Pioneering Quantum Beam Application by Osaka University and the SPRING program by Japan Science and Technology Agency.

References

- [1] Nguyen, H. L., Horton, P. N., Hursthouse, M. B., Legon, A. C. & Bruce, D. W. Halogen Bonding : A New Interaction for Liquid Crystal Formation. *J. Am. Chem. Soc.* 38, 16–17 (2004).
- [2] Matsuo, K., Yamaguchi, E. & Itoh, A. In Situ-Generated Halogen-Bonding Complex Enables Atom Transfer Radical Addition (ATRA) Reactions of Olefins. *J. Org. Chem.* 85, 10574–10583 (2020).
- [3] Wu, W. X., Liu, H. C. & Jin, W. J. Halogen Bonding Adsorbent Pyridine N-oxides for Iodine Capture in Water. *Chem. Eur. J.* 28, 1–5 (2022).
- [4] Politzer, P. & Murray, J. S. Halogen bonding: An interim discussion. *ChemPhysChem* vol. 14 278–294 (2013).
- [5] Cavallo, G. *et al.* The halogen bond. *Chem. Rev.* 116, 2478–2601 (2016).
- [6] Guérard, F. *et al.* Advances in the Chemistry of Astatine and Implications for the Development of Radiopharmaceuticals. *Acc. Chem. Res.* 54, 3264–3275 (2021).
- [7] Galland, N., Montavon, G., Le Questel, J. Y. & Graton, J. Quantum calculations of At-mediated halogen bonds: On the influence of relativistic effects. *New J. Chem.* 42, 10510–10517 (2018).
- [8] Feng, G., Evangelisti, L., Gasparini, N. & Caminati, W. On the $\text{Cl}\cdots\text{N}$ halogen bond: A rotational study of $\text{CF}_3\text{Cl}\cdots\text{NH}_3$. *Chem. Eur. J.* 18, 1364–1368 (2012).
- [9] Guo, N. *et al.* Experimental and computational evidence of halogen bonds involving astatine. *Nat. Chem.* 10, 428–434 (2018).
- [10] Liu, L. *et al.* An expanded halogen bonding scale using astatine. *Chem. Sci.* 12, 10855–10861 (2021).
- [11] Serov, A. *et al.* Adsorption interaction of astatine species with quartz and gold surfaces. *Radiochim. Acta* 99, 593–599 (2011).
- [12] Graham, D. The characterization of physical adsorption systems. II. The effects of attractive interaction between adsorbed molecules. *J. Phys. Chem.* 58, 869–872 (1954)
- [13] Lee, C., Parrillo, D. J., Gorte, R. J. & Farneth, W. E. Relationship between differential heats of adsorption and Bronsted acid strengths of acidic zeolites: H-ZSM-5 and H-mordenite. *J. Am. Chem. Soc.* 118, 3262–3268 (1996).
- [14] Erdélyi, M. Halogen bonding in solution. *Chem. Soc. Rev.* 41, 3547–3557 (2012).
- [15] Kalambet, Y., Kozmin, Y., Mikhailova, K., Nagaev, I. & Tikhonov, P. Reconstruction of chromatographic peaks using the exponentially modified Gaussian function. *J. Chromatogr. A* 25, 352–356 (2011).
- [16] M. J. Frisch, G. W. Trucks, H. B. Schlegel, G. E. Scuseria, M. A. Robb, J. R. Cheeseman, G. Scalmani, V. Barone, G. A. Petersson, H. Nakatsuji, X. Li, M. Caricato, A. V. Marenich, J. Bloino, B. G. Janesko, R. Gomperts, B. Mennucci, H. P. Hratchian, J. V. Gaussian 16, Revision C.01. (2016).
- [17] Roy Dennington, Todd A. Keith, and J. M. M. GaussView, Version 6.1. (2016).
- [18] Chai, J. Da & Head-Gordon, M. Long-range corrected hybrid density functionals with damped atom-atom dispersion corrections. *Phys. Chem. Chem. Phys.* 10, 6615–6620 (2008).
- [19] Dunning, T. H. Gaussian basis sets for use in correlated molecular calculations. I. The atoms boron through neon and hydrogen. *J. Chem. Phys.* 90, 1007–1023 (1989).
- [20] Kendall, R. A., Dunning, T. H. & Harrison, R. J. Electron affinities of the first-row atoms revisited. Systematic basis sets and wave functions. *J. Chem. Phys.* 96, 6796–6806 (1992).
- [21] Woon, D. E. & Dunning, T. H. Gaussian basis sets for use in correlated molecular calculations. III. The atoms aluminum through argon. *J. Chem. Phys.* 98, 1358–1371 (1993).
- [22] Godbout, N., Salahub, D. R., Andzelm, J. & Wimmer, E. Optimization of Gaussian-type basis sets for local spin density functional calculations. Part I. Boron through neon, optimization technique and validation. *Can. J. Chem.* 70, 560–571 (1992).
- [23] Sosa, C. *et al.* A local density functional study of the structure and vibrational frequencies of molecular transition-metal compounds. *J. Phys. Chem.* 96, 6630–6636 (1992).
- [24] Simon, S., Duran, M. & Dannenberg, J. J. How does basis set superposition error change the potential surfaces for hydrogen-bonded dimers? *J. Chem. Phys.* 105, 11024–11031 (1996).
- [25] Miertuš, S., Scrocco, E. & Tomasi, J. Electrostatic inter-

- action of a solute with a continuum. A direct utilization of AB initial molecular potentials for the prediction of solvent effects. *Chem. Phys.* 55, 117–129 (1981).
- [26] Greene, S. A. & Pust, H. The determination of heats of adsorption by gas-solid chromatography. *J. Phys. Chem.* 62, 55–58 (1958).
- [27] Hogan, S. W. L. & van Mourik, T. Halogen bonding in mono- and dihydrated halobenzene. *J. Comput. Chem.* 40, 554–561 (2019).
- [28] Thalladi, V. R. *et al.* C-H...F interactions in the crystal structures of some fluorobenzenes. *J. Am. Chem. Soc.* 120, 8702–8710 (1998).
- [29] Bramlett, T. A. & Matzger, A. J. Halogen Bonding Propensity in Solution: Direct Observation and Computational Prediction. *Chem. Eur. J.* 27, 15472–15478 (2021).
- [30] Inuzuka, K., Ito, M. & Imanishi, S. Effect of Solvent on Carbonyl Stretching Frequency of Ketones. *Bull. Chem. Soc. Jpn.* 34, 467–471 (1961).
- [31] Tsuzuki, S., Wakisaka, A., Ono, T. & Sonoda, T. Magnitude and origin of the attraction and directionality of the halogen bonds of the complexes of C₆F₅X and C₆H₅X (X=I, Br, Cl and F) with pyridine. *Chem. Eur. J.* 18, 951–960 (2012).
- [32] Stilić, V., Grgurić, T., Piteša, T., Nemeč, V. & Cinčić, D. Bifurcated and Monocentric Halogen Bonds in Cocrystals of Metal(II) Acetylacetonates with p-Dihalo-tetrafluorobenzenes. *Cryst. Growth Des.* 19, 1245–1256 (2019).